

Grain size and its relation to tensile strength of Nb₃Sn compound in bronze-processed multi-filamentary superconducting materials

SHOJIRO OCHIAI, KOZO OSAMURA, TOSHIHIRO UEHARA
Department of Metallurgy, Kyoto University, Sakyo-ku, Kyoto 606, Japan

The grain size and room-temperature tensile strength of Nb₃Sn compound were studied over wide ranges of annealing temperature and time using thin and thick multi-filamentary superconducting composite materials. The strength of Nb₃Sn compound in thick specimens was lower than that in thin specimens at any heat treatment. This result was accounted for by the existence of extra-coarse grains in thick specimens. It was found that the strength of Nb₃Sn compound is nearly proportional to the inverse square root of the grain size.

1. Introduction

The Nb₃Sn compound is known as one of the most promising superconducting materials. This compound is, however, very brittle and fractures at low strains, which gives serious consequences when an external load is applied and also gives a limit of strain tolerance in the superconducting properties [1–4]. Therefore it is strongly desirable to study the fracture behaviour and strength of this compound.

In our former work [5], the room-temperature tensile behaviour of the Nb₃Sn layer in bronze-processed multi-filamentary superconducting composite materials has been investigated over wide ranges of the factors of specimen size, annealing temperature and time. It was found that the strength of the Nb₃Sn layer estimated on the basis of the rule of mixtures [6, 7] decreases with increasing specimen size, annealing temperature and time. In later work using a given specimen size [8] it was found that the strength of this compound decreases with increasing grain size, and also that the relation of the strength to the grain size could be expressed empirically by an equation of the Hall–Petch [9, 10] type. In this work, the reason why the strength decreased with increasing annealing temperature and time was well understood since the grain size increased with increasing annealing temperature and time.

There still remains a question why the strength of the compound decreases with increasing specimen size. The aim of the present paper is to study the structure and strength of the Nb₃Sn compound in bronze-processed multi-filamentary composite materials by changing the specimen size, and to determine the reason why the strength of the compound becomes low when the specimen size becomes large.

2. Experimental procedure

The specimens employed in the present study were multi-filamentary composites supplied as the Japanese Standard Reference Sample for the superconducting materials group of the 1983–1985 energy research

programme of the Ministry of Education, Science and Culture of Japan. Two kinds of composite specimen were used in this study. The only difference between them was the diameter of the composite as a whole, d_c (0.31 and 2.60 mm). In this paper, the composite specimens with $d_c = 0.31$ and 2.60 mm are named as S1 and S3, respectively, as in our former works [5]. The S1 and S3 specimens are geometrically similar, having the same number of niobium filaments and the same volume fractions of niobium filaments, niobium barrier, Cu–Sn matrix and pure copper as a stabilizer. All specimens were composed of 745 niobium filaments in Cu–13 wt % Sn alloy, surrounded with a niobium barrier and then pure copper. The bronze and copper to non-copper ratios were 2 and 0.445, respectively, in both S1 and S3 specimens. The diameters of the niobium filaments in S1 and S3 specimens were, on average, 5 and 42 μm , respectively.

The experimental procedure was the same as that shown in our former papers [5, 8]. As the data of the earlier work were available, further experiments were carried out only for shorter and more prolonged annealing times at annealing temperatures of 973 and 1073 K. The present data, together with the former ones, cover the annealing periods of 17.3 to 4320 ksec at 973 and 1073 K for both S1 and S3 specimens. The volume fractions of Nb₃Sn, niobium and Cu–Sn were investigated with the SEM and electron probe microanalysis (EPMA). Tensile test was carried out with an Instron type tensile machine at room temperature at a strain rate of $3.33 \times 10^{-3} \text{ sec}^{-1}$. The fractured specimens were observed with the SEM to determine the morphology of the Nb₃Sn layer. The tensile strength of the Nb₃Sn layer was obtained by the procedure shown in our former work [5, 8]. The grain size of the Nb₃Sn compound was measured from the fracture surface observed with the SEM. First the one-dimensional grain size was obtained with the linear-line-intercept method and then it was converted to the three-dimensional one by multiplying by 1.56 under an approximation that the grain is spherical.

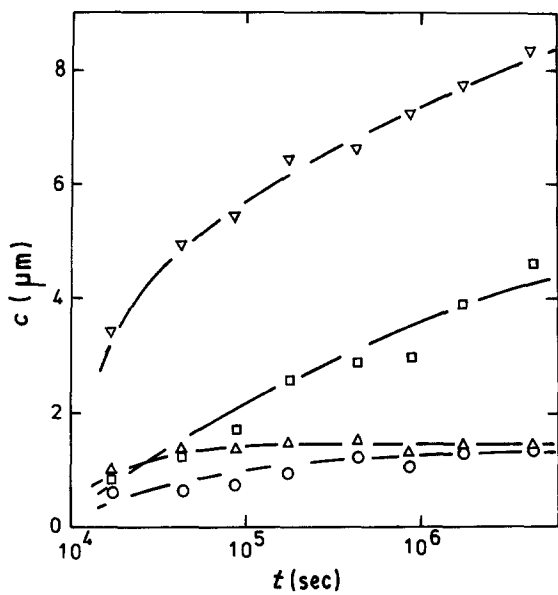


Figure 1 Variation of c as a function of t : (○) S1, 973 K; (□) S3, 973 K; (△) S1, 1073 K; (▽) S3, 1073 K.

3. Results and discussion

3.1. Thickness and volume fraction of Nb_3Sn layer

The thickness c of the Nb_3Sn layer increased with increasing temperature T and time t , as shown in Fig. 1. The c of the S1 specimens increased with increasing t and reached nearly $1.4\ \mu\text{m}$, remaining nearly constant for longer t . On the other hand, the c of the S3 specimens did not reach a constant value even for prolonged annealing time within the range investigated.

Fig. 2 shows the variation of the volume fraction of Nb_3Sn layer, $V_{\text{Nb}_3\text{Sn}}$, which is the sum of the volume fractions of the Nb_3Sn formed on niobium filaments and at the niobium barrier. The $V_{\text{Nb}_3\text{Sn}}$ of the S1 specimens showed a saturation for prolonged annealing

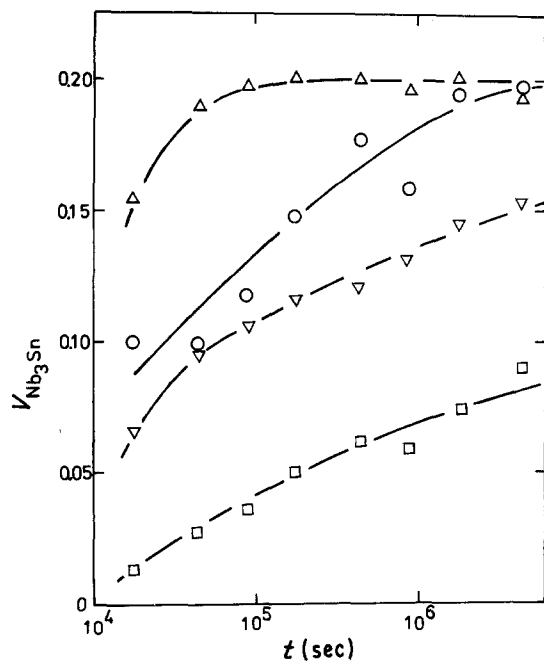


Figure 2 Variation of $V_{\text{Nb}_3\text{Sn}}$ as a function of t : (○) S1, 973 K; (□) S3, 973 K; (△) S1, 1073 K; (▽) S3, 1073 K.

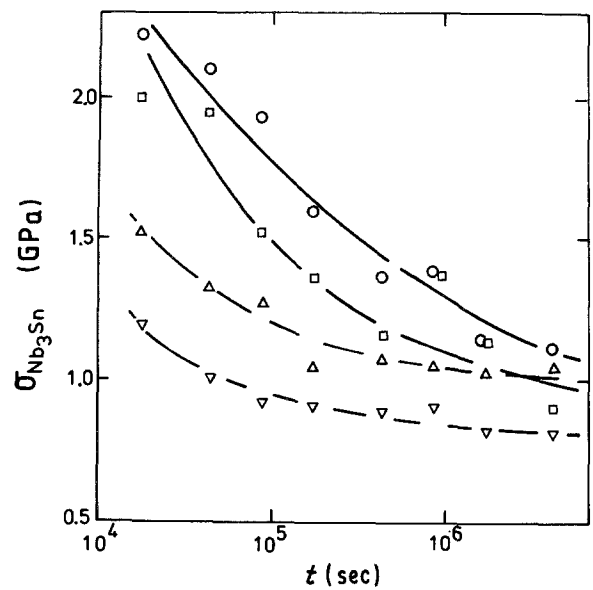


Figure 3 Variation of $\sigma_{\text{Nb}_3\text{Sn}}$ as a function of t : (○) S1, 973 K; (□) S3, 973 K; (△) S1, 1073 K; (▽) S3, 1073 K.

times, while that of the S3 specimens did not show it within the range of this work. This means that elemental tin had been consumed to form Nb_3Sn in the S1 specimens but it still existed in the S3 specimens for prolonged times.

3.2. Tensile strength of Nb_3Sn layer

3.2.1. Difference in tensile strength of Nb_3Sn layer between thin and thick specimens

Fig. 3 shows the variation of the strength of the Nb_3Sn layer, $\sigma_{\text{Nb}_3\text{Sn}}$, as a function of t . There are two distinct features:

(i) The higher the annealing temperature and the longer the annealing time, the lower becomes the $\sigma_{\text{Nb}_3\text{Sn}}$ for both S1 and S3 specimens.

(ii) The $\sigma_{\text{Nb}_3\text{Sn}}$ in thin S1 specimens is higher than that in thick S3 specimens at any annealing temperature and time.

The feature (i) can be attributed to the fact that grain size d becomes large with increasing annealing temperature and time, as ascertained previously [8].

To account for the feature (ii), two possibilities were considered in this work. Generally, brittle materials have a characteristic that the thinner the materials, the stronger they become, since they have fewer defects [11, 12]. This is the first possibility. If the present Nb_3Sn layer had this characteristic, it would be easy to understand why the thin Nb_3Sn layer in the thin S1 specimens is stronger than the thick Nb_3Sn layer in the thick S3 specimens for a given heat-treatment. To examine this possibility, $\sigma_{\text{Nb}_3\text{Sn}}$ was plotted against thickness c . Fig. 4 shows the result, where the values shown by square symbols were taken from S1 specimens annealed at 1123, 1173, 1223 and 1273 K for 86 ksec to obtain large grain size after having been annealed at 973 K for 432 ksec [8]. Contrary to the expectation that the $\sigma_{\text{Nb}_3\text{Sn}}$ of the S1 specimens would be higher than that of S3 specimens at a given c , the

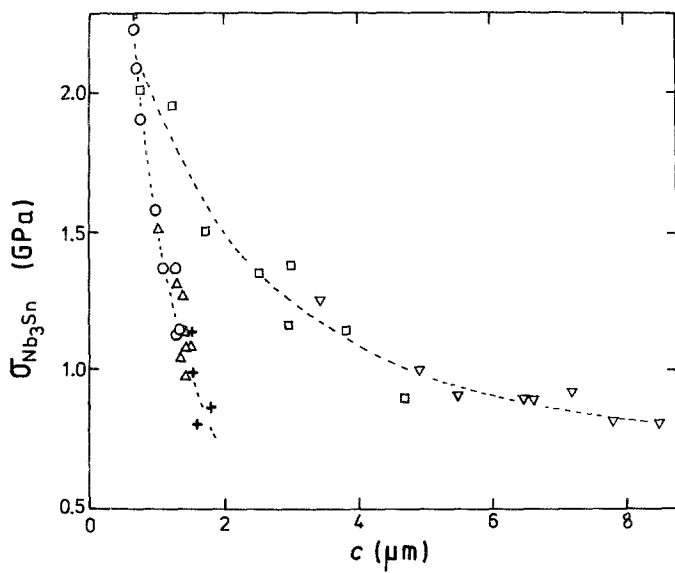


Figure 4 $\sigma_{\text{Nb}_3\text{Sn}}$ plotted against c : (O) S1, 973 K; (\square) S3, 973 K; (Δ) S1, 1073 K; (∇) S3, 1073 K; (+) S1 annealed at 1123, 1173, 1223 and 1273 K for 86 ksec after having been annealed at 973 K for 432 ksec [8].

former was lower than the latter. Thus the possibility mentioned above was disproved.

The next possibility is that the structure of the Nb_3Sn in the S3 specimens is different from that in the S1 specimens. The structure, especially the grain size of the Nb_3Sn layer, was therefore studied in detail, since for the S1 specimens it has been demonstrated that the strength of the Nb_3Sn layer had a strong dependency on grain size [8].

3.2.2. Difference in grain size of Nb_3Sn layer between thin and thick specimens and its influence on the strength

The fracture morphology of the Nb_3Sn layer was quite different between the S1 and S3 specimens. Fig. 5 shows typical examples of the fracture surface of the Nb_3Sn layer in S1 annealed at 973 K for 432 ksec (Fig. 5a) and 1073 K for 1730 ksec (Fig. 5b), and for S3 annealed at 1073 K for 432 ksec (Fig. 5c) and

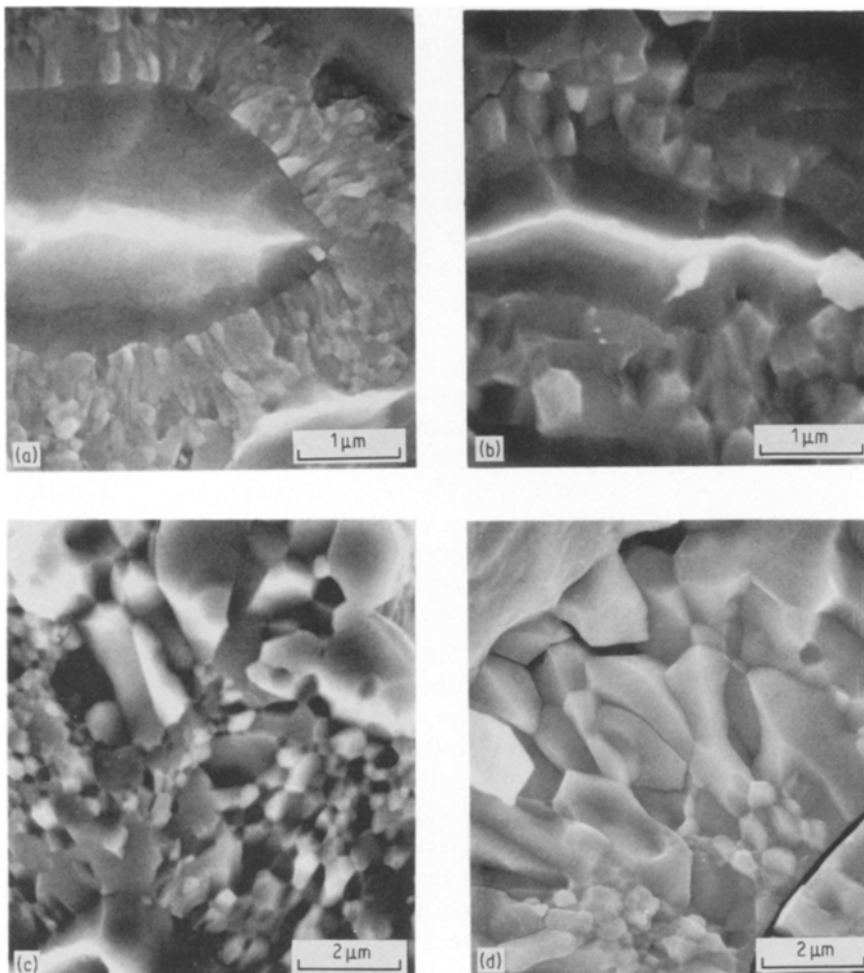


Figure 5 Fracture surfaces of the Nb_3Sn layer: (a) S1 specimen annealed at 973 K for 432 ksec, (b) S1 specimen at 1073 K for 1730 ksec, (c) S3 specimen at 1073 K for 432 ksec and (d) S3 specimen at 1073 K for 1730 ksec, showing extra-coarse grains in the S3 specimens (c, d) which are not found in the S1 specimens (a, b).

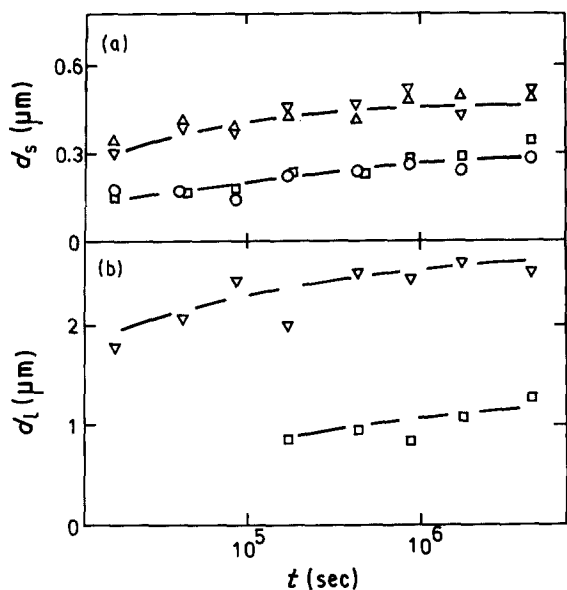


Figure 6 (a) Average measured values of grain size in the region of small grains, d_s , in the S3 specimens, together with the average grain size measured in the S1 specimens d_{ave} for comparison ((\square) d_s in S3, 973 K; (∇) d_s in S3, 1073 K; (\circ) d_{ave} in S1, 973 K; (\triangle) d_{ave} in S1, 1073 K), and (b) those in the region of extra coarse grains, d_l , in the S3 specimens ((\square) S3, 973 K; (∇) S3, 1073 K).

1073 K for 1730 ksec (Fig. 5d). In the S1 specimens, there was a slight tendency for the grain size of the Nb_3Sn layer to increase with increasing distance from the Nb– Nb_3Sn interface. However, the sizes of the grains were not much different from each other, compared with the difference in size in the S3 specimens. In the S3 specimens, very coarse grains were found as shown in Figs 5c and d. Such coarse grains in the S3 specimens were observed for $t \geq 173$ ksec at 973 K annealing and for $t \geq 17.3$ ksec at 1073 K annealing. The average grain size was then measured in both regions of small grains, d_s , and extra large grains, d_l , separately in the S3 specimens when such large grains were observed. Fig. 6 shows the average values of d_s (Fig. 6a) and d_l (Fig. 6b) in the S3 specimens together with those measured in the S1 specimens (plotted in Fig. 6a). It is interesting that the d_s values of the S3 specimens are nearly the same as the average grain size in the S1 specimens for any heat-treatment. This might indicate that, if no coarse grains arose, the average grain size would be determined only by the annealing temperature and time. At present, the reason why very coarse grains are formed in the thick specimens is unknown.

As it has been established that the relation of the strength of the Nb_3Sn layer to grain size in the S1 specimens can be empirically expressed by the Hall–Petch type of equation [8], the value of σ_{Nb_3Sn} was plotted against $d^{-1/2}$, where d_s was taken as the grain size d for the S1 specimens and S3 specimens in which no coarse grains were observed and d_l was taken as d for the S3 specimens in which coarse grains were observed. Fig. 7 shows the result. Although a wide scatter is found, the data points approximately fall on a straight line. In Fig. 7, the average grain size d_{ave} was used as d when extra-coarse grains did not exist and d_l was used as d when they existed. It is, however, not sure that d_{ave} can be compared with d_l directly. Then, as

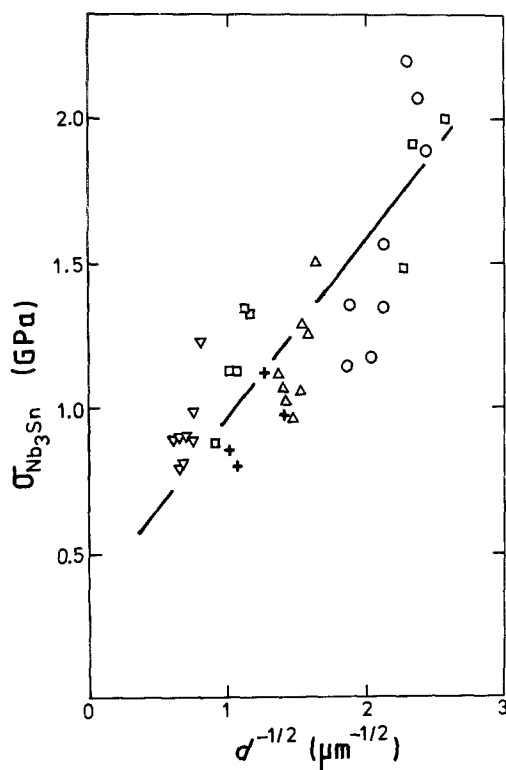


Figure 7 σ_{Nb_3Sn} plotted against $d^{-1/2}$, where average grain size was taken as d for the S1 specimens and the S3 specimens in which extra-coarse grains were not found, and d_l was taken as d for the S3 specimens in which extra-coarse grains were found. (\circ) S1, 973 K; (\square) S3, 973 K; (\triangle) S1, 1073 K; (∇) S3, 1073 K; (+) S1 annealed at 1123, 1173, 1223 and 1273 K for 86 ksec after having been annealed at 973 K for 432 ksec [8].

it was expected from the fracture surface of the Nb_3Sn layer that coarser grains exist near the interface between the Nb_3Sn and the Cu–Sn matrix even in the S1 specimens which have no extra-coarse grains, side views of the Nb_3Sn layer were observed by etching away the copper, niobium barrier and Cu–Sn matrix. Fig. 8 shows an example of the side view of the Nb_3Sn layer of an S1 specimen annealed at 1073 K for 864 ksec (Fig. 8a), together with the fracture surface of the same specimen (Fig. 8b) for comparison, and the side view of an S3 specimen under the same heat-treatment (Fig. 8c) for comparison, too. The specimen of Fig. 8c observed after tensile test shows also the fracture path, indicating that the fracture proceeds not only intergranularly but also transgranularly.

Comparing Figs 8a to c with each other, it is evident that the average grain size in the side surface of the S1 specimen (Fig. 8a) is larger than that in the fracture surface (Fig. 8b), and that the grain size in the side surface of the S1 specimen is smaller than that in the S3 specimen (Fig. 8c) under the same heat-treatment. The grain sizes in the side surfaces of the S3 specimens were nearly the same as the sizes of the extra-coarse grains in the fracture surface. The average grain size in the side surface was then measured as d_l for the specimens without extra-coarse grains. Fig. 9 shows the variation of d_l as a function of t for the S1 specimens, together with that of d_{ave} for comparison. The difference between d_{ave} and d_l is small for short annealing times but it becomes large with increasing t . The value of σ_{Nb_3Sn} was plotted against $d_l^{-1/2}$ as shown in Fig. 10.

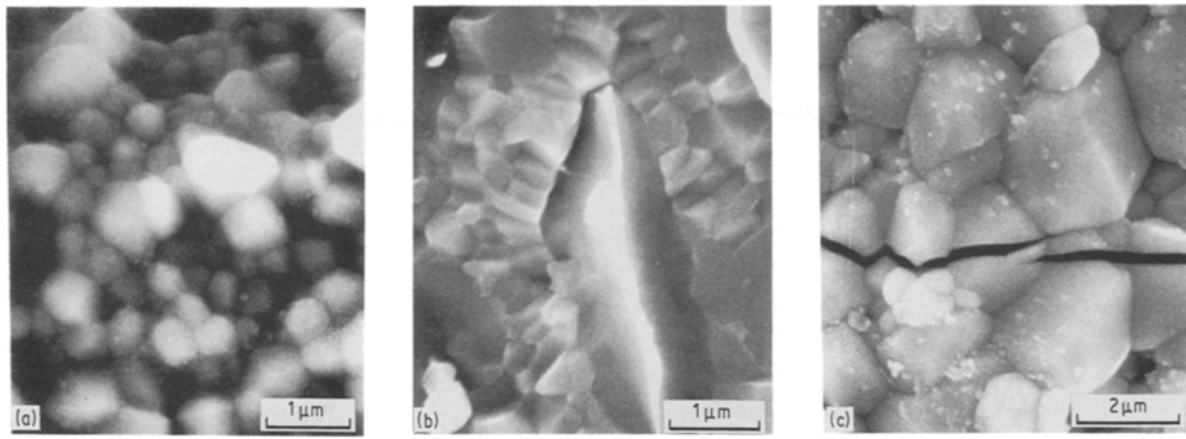


Figure 8 An example of the side view of the Nb₃Sn layer in (a) S1 specimen annealed at 1073 K for 864 ksec, together with (b) the fracture surface of the same specimen for comparison, and (c) the side view of the layer in an S3 specimen given the same heat-treatment.

Both Figs 7 and 10 can give the same conclusion in the point that the data points approximately fall on a straight line. The difference between Figs 7 and 10 is that the scatter in Fig. 10 becomes smaller than that in Fig. 7.

The results shown in Fig. 10 imply that the strength of the Nb₃Sn layer in both S1 and S3 specimens is proportional to the inverse square root of the grain size when the size of coarse grains is employed as the representative grain size. From the present result, the reason why the Nb₃Sn layer becomes weak when the specimen thickness becomes large can be accounted for by the existence of extra-coarse grains in thick specimens.

The reason why $\sigma_{\text{Nb}_3\text{Sn}}$ is nearly proportional to $d_i^{-1/2}$ is not known at present. One possible reason is that microscopic plastic flow or dislocation movement occurs even at room temperature so that a crack is nucleated by a dislocation pile-up process against grain boundaries [9, 10, 13]. However, it is unknown whether microscopic plastic flow occurs or not at room temperature, although it has been known that plastic flow occurs under high hydrostatic pressure at room temperature and also under zero and ambient

pressure at elevated temperatures [14–16]. Another possible reason is that a crack is nucleated by the fracture of a grain boundary, so that the grain size is nearly equal to the crack length. According to this concept, Griffith theory [17] may be useful, since it too gives a relation that $\sigma_{\text{Nb}_3\text{Sn}}$ is proportional to $d_i^{-1/2}$ if the crack length is proportional to the grain size. At present, either of the above possibilities can be argued. In order to clarify the reason why $\sigma_{\text{Nb}_3\text{Sn}}$ is nearly proportional to $d_i^{-1/2}$, further study is needed.

4. Conclusions

The grain size and room-temperature tensile strength of the Nb₃Sn layer in bronze-processed multi-filamentary superconducting composite materials were studied. The strength of the Nb₃Sn layer in thick specimens

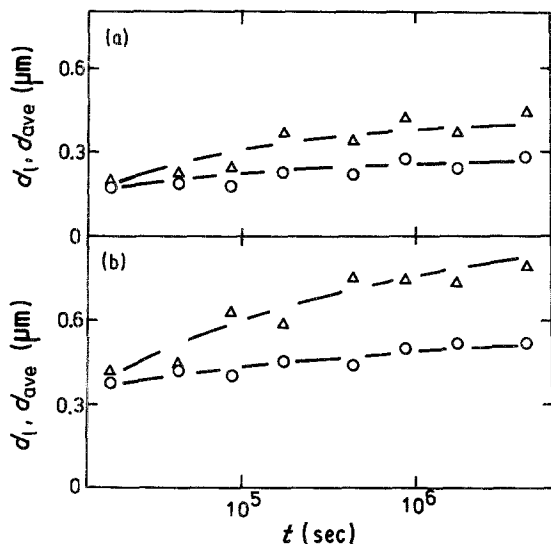


Figure 9 Variation of (Δ) d_i as a function of t of the S1 specimens, together with that of (\circ) d_{ave} for comparison; (a) 973 K, (b) 1073 K.

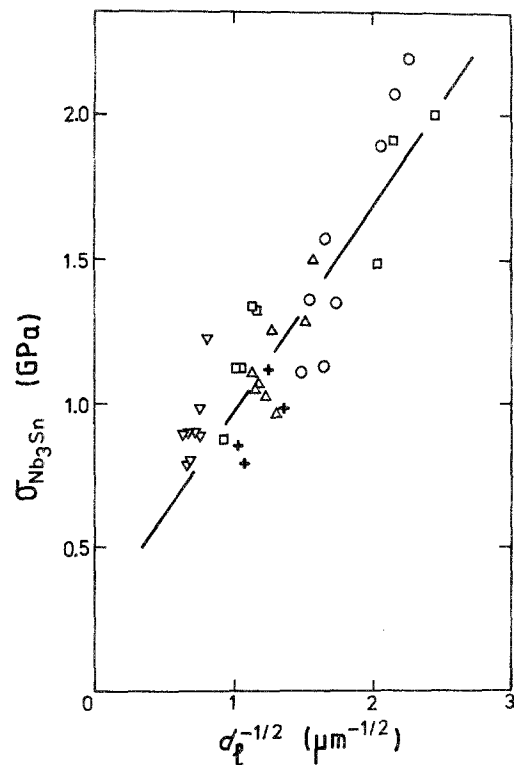


Figure 10 $\sigma_{\text{Nb}_3\text{Sn}}$ plotted against $d_i^{-1/2}$; (\circ) S1, 973 K; (\square) S3, 973 K; (Δ) S1, 1073 K; (∇) S3, 1073 K; (+) S1 annealed at 1123, 1173, 1223 and 1273 K for 86 ksec after having been annealed at 973 K for 432 ksec [8].

was lower than that in thin specimens for any heat-treatment. This was accounted for by the existence of extra-coarse grains in the thick specimens. It was found that the strength of the Nb₃Sn layer is nearly proportional to inverse root grain size.

Acknowledgement

The authors wish to express their gratitude to Messrs I. Nakagawa and T. Unesaki at Kyoto University for their help in the SEM and EPMA studies. They also express their gratitude to the Ministry of Education, Science and Culture of Japan for a grant-in-aid for energy research (No. 610 500 33).

References

1. J. W. EKIN, in "Superconducting Materials Science — Metallurgy, Fabrication and Applications", edited by S. Foner and B. B. Schwarz (Plenum, New York, 1981) p. 455.
2. G. RUPP, in "Filamentary A15 Superconductors", edited by M. Suenaga and A. F. Clark (Plenum, New York, 1980), p. 155.
3. T. LUHMAN and D. O. WELCH, *ibid.* p. 171.
4. T. LUHMAN, M. SUENAGA, D. O. WELCH and K. KAIHO, *IEEE Trans. Mag.* **MAG-15** (1979) 699.
5. S. OCHIAI, K. OSAMURA and T. UEHARA, *J. Mater. Sci.* **21** (1986) 1027.
6. D. L. McDANIELS, R. W. JECH and J. W. WEETON, *Trans. Met. Soc. AIME* **233** (1965) 636.
7. A. KELLY and W. R. TYSON, *J. Mech. Phys. Solids* **13** (1965) 329.
8. S. OCHIAI, T. UEHARA and K. OSAMURA, *J. Mater. Sci.* **21** (1986) 1020.
9. E. O. HALL, *Proc. Phys. Soc.* **64B** (1951) 747.
10. N. J. PETCH, *J. Iron Steel Inst.* **173** (1953) 25.
11. W. WEIBULL, *J. Appl. Mech.* **18** (1951) 293.
12. A. De S. JAYATILAKA and K. TRUSTRUM, *J. Mater. Sci.* **12** (1977) 1426.
13. A. J. STROH, *Adv. Phys.* **6** (1957) 418.
14. R. N. WRIGHT, *Met. Trans.* **8A** (1977) 2024.
15. L. R. EISENSTATT and R. N. WRIGHT, *ibid.* **11A** (1980) 1131.
16. J. B. CLARK and R. N. WRIGHT, *ibid.* **14A** (1983) 2295.
17. A. A. GRIFFITH, *Phil. Trans. R. Soc.* **A221** (1920) 163.

*Received 4 August
and accepted 22 September 1986*